Quantum Science and Technology

PAPER

Joint subnatural-linewidth and single-photon emission from resonance fluorescence

J C López Carreño[1,2] , E Zubizarreta Casalengua[1] , F P Laussy[2,3] and E del Valle[1]

[1] Departamento de Física Teórica de la Materia Condensada, Universidad Autónoma de Madrid, E-28049 Madrid, Spain
[2] Faculty of Science and Engineering, University of Wolverhampton, Wulfruna St., Wolverhampton WV1 1LY, United Kingdom
[3] Russian Quantum Center, Novaya 100, 143025 Skolkovo, Moscow Region, Russia

E-mail: elena.delvalle.reboul@gmail.com

Abstract

Resonance fluorescence—the light emitted when exciting resonantly a two-level system—is a popular quantum source as it seems to inherit its spectral properties from the driving laser and its statistical properties from the two-level system, thus providing a subnatural-linewidth single-photon source (SPS). However, these two qualities do not actually coexist in resonance fluorescence, since an optical target detecting these antibunched photons will either be spectrally broad itself and not benefit from the spectrally narrow source, or match spectrally with the source but in this case the antibunching will be spoiled. We first explain this failure through a decomposition of the field-emission and how this gets affected by frequency resolution. We then show how to restore the sought joint subnatural linewidth and antibunched properties, by interfering the resonance fluorescence output with a coherent beam. We finally discuss how the signal that is eventually generated in this way features a new type of quantum correlations, with a plateau of antibunching which suppresses much more strongly close photon pairs. This introduces a new concept of perfect SPS.

1. Introduction

Resonance fluorescence has always been a central topic in quantum optics, being the simplest nontrivial quantum light source: a two-level system driven coherently close to, or at, its resonance [1–10]. Early on, it has been recognised as a single-photon source (SPS) that should exhibit perfect antibunching, that is, a complete suppression of photon coincidences. Intuitively, this is because no photon can be emitted (or detected by an ideal detector) at the same time as another one, due to the finite reloading time of the system after an emission. This experimental observation made resonance fluorescence, in fact, the first system to fully prove the quantisation of light [8], by violating the classical Cauchy–Schwarz inequality for the intensity–intensity correlations in time. This has since been tested and confirmed throughout the history of the field in a variety of platforms [11–18]. It also created an obvious incentive of perfecting this source of single-photons for applications, since a SPS is a crucial component of quantum technology in most platforms, including cold atoms [19–21], ions [22–24], molecules [25–28], semiconductor quantum dots [29–37], superconducting circuits [17, 38–41], nitrogen vacancies [42–44], and still others. Recent years have been particularly fruitful towards the implementation of an ideal SPS ripe for commercial development and industrial applications [45–51]. In this respect, resonance fluorescence appears to be among the best contenders. Together with its sub-Poissonian statistics, it also has a very strong emission rate thanks to the efficient coherent driving, and, in contrast to incoherent driving that results in power broadening, it can be operated in the so-called *Heitler regime* [1] where its spectral width is actually narrower than the natural linewidth of the emitter, being instead given by the driving laser. This led to the claim of the emission as an elastic scattering (i.e., Rayleigh) peak, which retains the coherence as well as spectral width of the laser [52, 53], and the antibunching of the two-level system [54].

Resonance fluorescence is therefore a precious resource, since all these three attributes are precisely those demanded by the prospective quantum circuits for the technology of tomorrow: antibunching to deal with

quantum states, brightness to provide a strong signal and narrow spectral width to have indistinguishable photons. These qualities were first explored with a single trapped ion [54] and more recently exploited with a single semiconductor quantum dot [46, 55–59] which is still under active development. All these studies follow a similar trend: they analyse spectral properties with the best available spectral resolution on the one hand, and then the statistical properties (the second-order correlation function) with the best available temporal resolution on the other hand. These constitute two different experiments, providing excellent results in both cases and seemingly fulfilling the ideal scenario we have just described: perfect antibunching of spectrally narrow sources. However, one should contrast these qualities *together*, that is to say, simultaneously. One is ultimately interested not in how well the source performs when considering one aspect or the other in isolation, but how an optical target that is excited by the source will 'perceive' these photons. Such a target will have a spectral width Γ and couple to the source accordingly, preventing it to see the photon statistics with an independent time resolution, that is needed to extract the best antibunching. Therefore, to properly describe the SPS, one needs to study the spectral and statistical properties of resonance fluorescence as detected in one and the same experimental setup, including the Heisenberg time and frequency uncertainties.

Doing so, we find that for resonance fluorescence, subnatural linewidth of the emission is not compatible with a simultaneous strong antibunching. The observed (or detected) linewidth of the Rayleigh peak is broadened by the spectral resolution Γ. Keeping this broadening below the natural two-level system decay rate γ_σ spoils the antibunching and brings the statistics to the Poissonian limit. The expression for the filtered (or convoluted with the detector) second-order correlation function of resonance fluorescence at low driving is indeed known to be $g_a^{(2)} = [\gamma_\sigma/(\gamma_\sigma + \Gamma)]^2$, which goes to 1 as $\Gamma \rightarrow 0$ [60]. Antibunching is thus washed out by the large detector time uncertainty $1/\Gamma$. This incompatibility is shown for our problem at hand in rows (i), (ii) of figure 1.
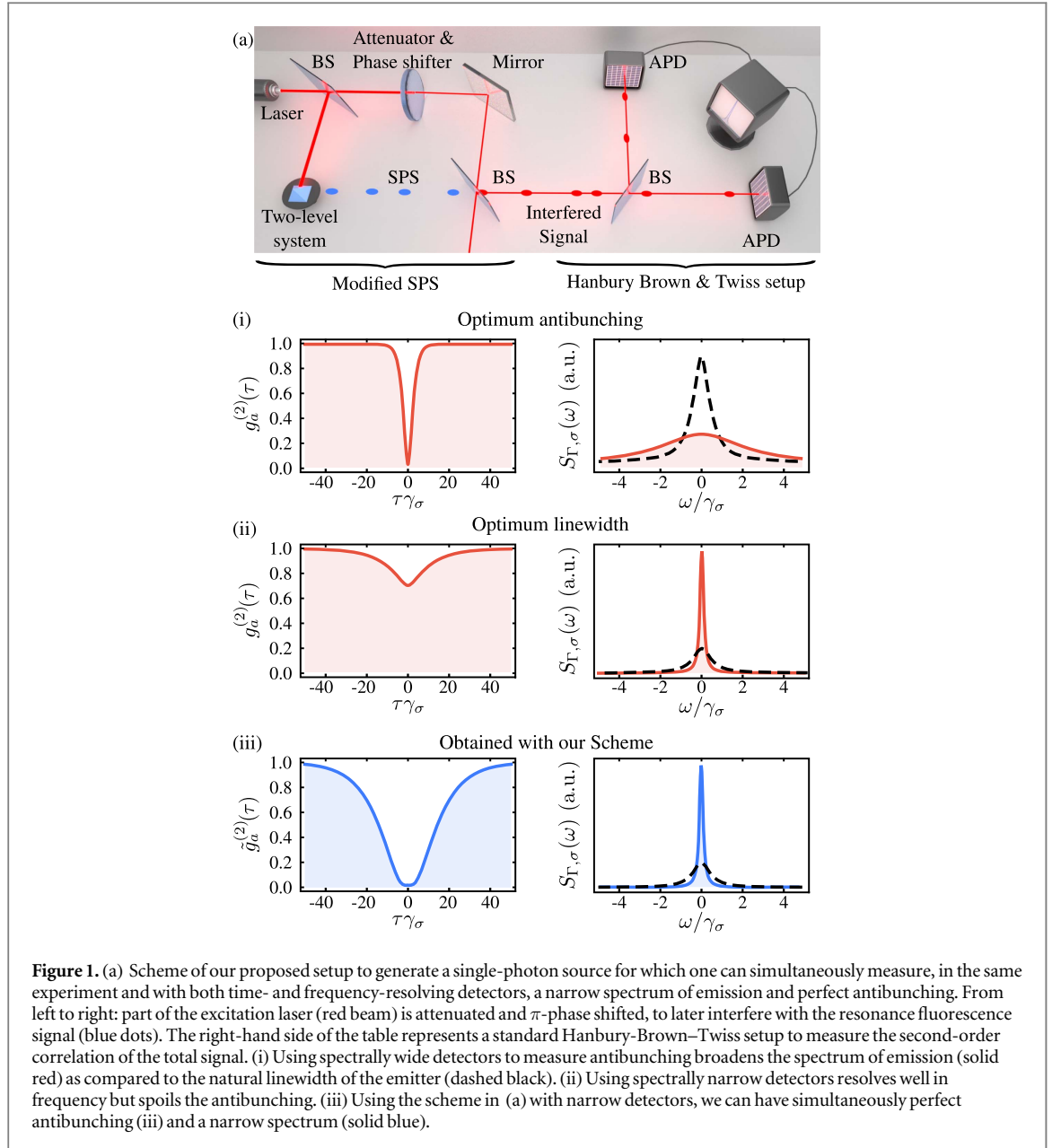
Although it does not work with resonance fluorescence per se, the intuition of the pioneering experiments [55, 56] to realise a subnatural-width antibunched source (implying, *simultaneously*), is not forbidden on fundamental grounds: one can imagine a source as spectrally narrow and antibunched as one wishes, merely by changing the timescale $(1/\gamma_\sigma)$. There is therefore no *a priori* reason why the initial claim could not be realised one way or the other.

In this text, we present a scheme to do that, that is, to provide perfect antibunching from resonance fluorescence without renouncing to subnatural linewidth. This is achieved, in contrast to previous works, so that the *same* detection setup measures *simultaneously* these two quantities: antibunching and narrow spectral width. We base our protocol on the understanding of such perfect antibunching as the result of destructive interference between the coherent and incoherent fractions of the emission: the coherently scattered photons and those that are absorbed and re-emitted [15]. The detector can then be seen as a filter that breaks the equilibrium between these two fractions, absorbing more coherent than incoherent light. We can thus restore this equilibrium since coherent light is easy to control. We propose to do so with a setup such as the one sketched in figure 1(a), where the coherent fraction in the resonance fluorescence signal is reduced by making it interfere with an external π-phase shifted laser beam, attenuated to the right proportion for the compensation to be perfect. We provide the exact (analytical) condition for this to occur as well as a full analysis of the spectral, statistical and intensity properties in terms of all the relevant parameters of the problem. We also show that, in fact, such a source goes even further and behaves more closely to an ideal SPS than would resonance fluorescence alone operating in a different timescale.

The rest of the paper is organised as follows: in section 2, we review the spectral and statistical properties of resonance fluorescence for ideal and realistic detectors, introducing the theoretical formalism as we do so, and we show how antibunching can be interpreted in terms of coherent and incoherent contributions to the second-order correlation function. In section 3, we present the setup to obtain perfect antibunching and high frequency resolution when considering realistic and simultaneous measurement of statistical and spectral properties, based on a complete theoretical description. We provide analytical expressions for the condition to be fulfilled, that could guide its experimental realisation. In section 4, we further analyse other important quantities to characterise the system, namely, the coherence time of the second-order correlation function and the emission rate of the source. Finally, in section 5, we conclude.

2. Antibunching in resonance fluorescence and the impact of detection

We consider the low driving regime of resonance fluorescence, or so-called *Heitler regime* [1]. In this scenario, the emitter is modelled as a two-level system with annihilation operator σ and is driven coherently with a weak laser of intensity Ω_σ. We consider the laser exactly at resonance with the two-level transition for simplicity but everything can be easily generalised to the close-to-resonance case by adding a detuning parameter. Importantly, we take into account the physical detection of resonance fluorescence. This is a central point of our approach as

Figure 1. (a) Scheme of our proposed setup to generate a single-photon source for which one can simultaneously measure, in the same experiment and with both time- and frequency-resolving detectors, a narrow spectrum of emission and perfect antibunching. From left to right: part of the excitation laser (red beam) is attenuated and π-phase shifted, to later interfere with the resonance fluorescence signal (blue dots). The right-hand side of the table represents a standard Hanbury-Brown–Twiss setup to measure the second-order correlation of the total signal. (i) Using spectrally wide detectors to measure antibunching broadens the spectrum of emission (solid red) as compared to the natural linewidth of the emitter (dashed black). (ii) Using spectrally narrow detectors resolves well in frequency but spoils the antibunching. (iii) Using the scheme in (a) with narrow detectors, we can have simultaneously perfect antibunching (iii) and a narrow spectrum (solid blue).

it allows us to consider the physical, self-consistent and complete description of the source. In particular, this accounts for the uncertainty in time and frequency of the detected photons [61]. Technically, this involves the integration of the convolution between the observable and a filtering function, which becomes exponentially difficult as the number of photons involved in the observable increases [62, 63]. Such a difficulty can be overcome if the detectors are considered as physical passive objects that receive the emission of the quantum source without disturbing it. This can be obtained when the detectors are described as harmonic oscillators that couple to the source either in the limit of vanishing coupling [64] or through the so-called *cascaded coupling* [65]. In either of these equivalent methods [66], the excitation is allowed to go from the quantum source to the detector while the feedback in the opposite direction is suppressed. Following these ideas, our detector is therefore considered as an harmonic oscillator, with bosonic annihilation operator a, and the full and self-consistent description of resonance fluorescence becomes an easy theoretical problem again. Indeed, the master equation describing this complete system is given by (we take $\hbar = 1$ from now on):

$$\partial_t \rho = \mathrm{i}[\rho, H] + \frac{\gamma_\sigma}{2}\mathcal{L}_\sigma \rho + \frac{\Gamma}{2}\mathcal{L}_a \rho. \tag{1}$$

The dissipation term $\mathcal{L}_c = 2c\rho c^\dagger - c^\dagger c\rho - \rho c^\dagger c$ is in the Lindblad form, with γ_σ and Γ being the decay rates of the two-level system and the detector, respectively. The parameter Γ provides the spectral width of the detector and its inverse, $1/\Gamma$, thus gives the temporal uncertainty of the detector. The Hamiltonian, $H = \Omega_\sigma(\sigma + \sigma^\dagger) + g(a^\dagger \sigma + \sigma^\dagger a)$, describes the laser driving the two-level system (with a parameter Ω_σ that we consider to be real

without loss of generality) and its coupling to the detector is taken as g (also real). We set the detector at resonance with both the laser and the two-level system.

One of the central quantities in this work is the second-order correlation function [67], typically defined, for a source with operator s in the steady state, as:

$$g_s^{(2)}(\tau) = \lim_{t \to \infty} \frac{\langle s^\dagger(t)(s^\dagger s)(t+\tau)s(t)\rangle}{[\langle s^\dagger s\rangle(t)]^2} = \frac{\langle s^\dagger(s^\dagger s)(\tau)s\rangle}{\langle s^\dagger s\rangle^2}. \tag{2}$$

We omit the time t in all expressions, which we consider to be large enough for the system to have reached the steady state. When the delay τ is omitted as well, it is implicitly assumed to be zero: $g_s^{(2)} = g_s^{(2)}(\tau = 0)$, which describes coincidences. We will also be considering the Nth-order correlation functions, but then always at zero time delay: $g_s^{(N)} = \langle s^{\dagger N} s^N\rangle / \langle s^\dagger s\rangle^N$.

Let us start by reviewing the spectral properties of this system with perfect frequency resolution [2, 68]. The details of the derivation can be found in appendix B. The normalised steady state spectrum of emission in the low driving regime, $\Omega_\sigma \ll \gamma_\sigma$, formally defined in equation (B.8), reads

$$S_\sigma(\omega) = (1 - K_2)\delta(\omega) + K_2 \frac{1}{\pi} \frac{\frac{\gamma_\sigma}{2}}{\left(\frac{\gamma_\sigma}{2}\right)^2 + \omega^2}, \tag{3}$$

where K_2 is given by, up to second order in the driving, $K_2 = 8\Omega_\sigma^2/\gamma_\sigma^2$. This is simply the superposition of a delta and a Lorentzian peaks, both centred at the laser frequency (at zero), with no width and γ_σ-width, respectively. The delta function term is the Rayleigh peak attributed to the elastic scattering of the laser photons by the two-level system while the Lorentzian term comes from the actual two-photon excitation and re-emission [69]. Note that in the linear regime and particularly in the limit $\Omega_\sigma \to 0$ and excluding second-order terms (which involve two-photon states in the detector), the spectrum of emission reduces to the delta function. That is, if one is interested in the spectral density of isolated one-photon events only, regardless of their time of arrival or their relation to other photons, the source is effectively providing photons as spectrally narrow as the laser (here infinitely narrow making the source perfectly monochromatic). However, if such photons are to be used in temporal relation with others, such as when considering their antibunching properties, then the second-order part of the spectrum must be taken into account. By having the frequency resolution below the natural emitter linewidth (in order to maintain a narrow spectrum to first order) one filters out part of the incoherent spectrum which determines its statistics. On the other hand, increasing the frequency resolution in order to increase temporal precision, broadens the spectrum. As a result, resolving antibunching spoils the subnatural linewidth of the source, and vice versa. To make this important point more quantitative, let us consider $g_a^{(N)}$ the Nth-order correlation function of resonance fluorescence as measured by a detector with both frequency and time resolution (set at resonance with the source). The expressions for a general laser driving strength exist but are bulky (see, for instance, the case $N = 2$ in equation (19b) of [70]). Here, since we are interested in the Heitler regime, it is enough to expand these expressions to the lowest order in the driving, which is, for $\langle a^{\dagger N} a^N\rangle$, to order $O(\Omega_\sigma^{2N})$, as shown in appendix A with $\Omega_a = 0$. This allows us to generalise to all orders the expression for the correlations, that simply reduces to (for $N \geqslant 2$):

$$g_a^{(N)} = \prod_{k=1}^{N-1} \frac{\gamma_\sigma^2}{(\gamma_\sigma + k\Gamma)^2}. \tag{4}$$

We have already discussed the case $N = 2$ above. As expected, when $\Gamma \to \infty$, this expression recovers the perfect antibunching of the source itself, i.e., when the full emission is being detected without any frequency resolution: $\lim_{\Gamma \to \infty} g_a^{(N)} = g_\sigma^{(N)} = 0$ [64]. In the opposite limit of narrow frequency filtering, the result for a coherent field is obtained: $\lim_{\Gamma \to 0} g_a^{(N)} = 1$ for all N. With the present semi-classical model for the laser, which has zero linewidth (perfect first-order coherence), we do not recover the expected thermal value for photons of completely undetermined time of emission, i.e., $\lim_{\Gamma \to 0} g_a^{(N)} \neq N!$, because it is impossible to filter inside the laser width [60]. For a general intermediate Γ, the perfect antibunching needed for quantum applications, is spoiled: $0 < g_a^{(N)} \leqslant 1$. For instance, when filtering at the natural linewidth of the emitter $\Gamma = \gamma_\sigma$, we obtain a reduction of 25% in the antibunching ($g_a^{(2)} = 1/4$) and $\Gamma = \gamma_\sigma/3$ leads to $g_a^{(2)} = 0.56$. As a consequence, making use of the subnatural spectral width of such a SPS [56], which implies detecting its photon with some accuracy in time and frequency, or coupling its output light to an optical element with $\Gamma < \gamma_\sigma$, spoils its statistical properties. In summary, subnatural linewidth and antibunching are in contradiction for resonance fluorescence in its bare form. The system emits photons which one can choose to see, depending on the detection scheme, with the properties of the driving laser or of the emitter, but not simultaneously.

In order to address this discouraging issue, let us dive deeper into the mechanism that yields antibunching in resonance fluorescence when integrating over its full spectrum, with $\Gamma \to \infty$. This can be understood in terms of interfering fields: it has indeed been long known that the emission of a coherently driven two-level system can be expressed as a superposition of a coherent and a squeezed incoherent field [15, 71]. We apply a mean field

procedure and write $\sigma = \alpha + d$, with a mean coherent field $\alpha = \langle\sigma\rangle$ and d an operator for the quantum fluctuations characterised by $\langle d\rangle = 0$. The coherent field is the one that gives rise to the delta function in the spectrum of emission (3) while the Fourier transform of $\langle d^\dagger d(\tau)\rangle$ provides the Lorentzian peak, i.e., the incoherent part of the spectrum, that transforms into the Mollow triplet when the driving increases [2]. Working out $g_\sigma^{(2)}$ in term of this decomposition results in four contributions:

$$g_\sigma^{(2)} = 1 + \mathcal{I}_0 + \mathcal{I}_1 + \mathcal{I}_2, \tag{5}$$

that grow as powers of α:

$$\mathcal{I}_0 = \frac{\langle d^{\dagger 2} d^2\rangle - \langle d^\dagger d\rangle^2}{\langle n_\sigma\rangle^2} = |\alpha|^2 \frac{6\langle n_\sigma\rangle - 4|\alpha|^2}{\langle n_\sigma\rangle^2} - 1, \tag{6a}$$

$$\mathcal{I}_1 = 4\frac{\mathfrak{R}(\alpha^*\langle d^\dagger d^2\rangle)}{\langle n_\sigma\rangle^2} = 8|\alpha|^2 \frac{|\alpha|^2 - \langle n_\sigma\rangle}{\langle n_\sigma\rangle^2}, \tag{6b}$$

$$\mathcal{I}_2 = 2\frac{|\alpha|^2\langle d^\dagger d\rangle + \mathfrak{R}(\alpha^{*2}\langle d^2\rangle)}{\langle n_\sigma\rangle^2} = 2|\alpha|^2 \frac{\langle n_\sigma\rangle - 2|\alpha|^2}{\langle n_\sigma\rangle^2}. \tag{6c}$$
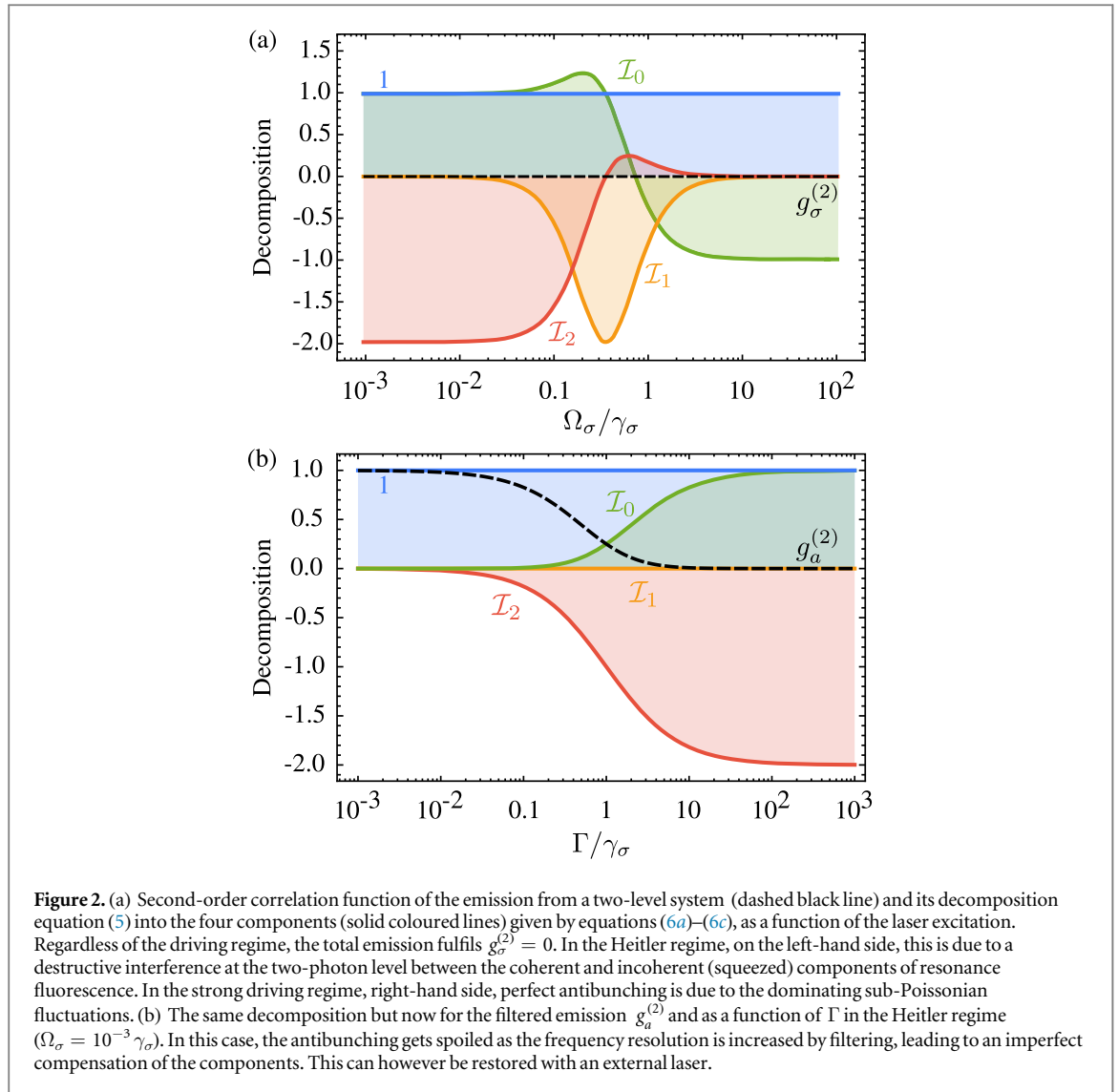
From the derivation in appendix B, we can further substitute $\alpha = -2i\Omega_\sigma\gamma_\sigma/(\gamma_\sigma^2 + 8\Omega_\sigma^2)$ and $\langle n_\sigma\rangle = \langle\sigma^\dagger\sigma\rangle = 4\Omega_\sigma^2/(\gamma_\sigma^2 + 8\Omega_\sigma^2)$. This decomposition is what one would obtain when performing a $g^{(2)}$ measurement on the output of a beam splitter, that would have σ as the associated output arm operator, with input fields α and d. This is the well known homodyne measurement, first suggested by Vogel [72, 73] to analyse the squeezing properties of signal d thanks to the controlled variation of a local oscillator α. The numerator of $\mathcal{I}_0$ in the left-hand side of equation (6a) is the normally ordered variance of the fluctuation intensity, i.e., $\langle:(\Delta n_d)^2:\rangle = \langle:n_d^2:\rangle - \langle n_d\rangle^2$ with $n_d = d^\dagger d$ and $\Delta n_d = n_d - \langle n_d\rangle$. Therefore, having $\mathcal{I}_0 < 0$ indicates sub-Poissonian statistics of the fluctuations, which, in turn, contributes to the sub-Poissonian statistics of the total field σ. The numerator of $\mathcal{I}_1$ in equation (6b) represents the normally ordered correlation between the fluctuation field-strength and intensity, $\langle d^\dagger d^2\rangle = \langle:\Delta d\Delta n_d:\rangle$, which have been referred to as *anomalous moments* [72, 73]. A squeezed-coherent state has such correlations. The numerator of the last component, $\mathcal{I}_2$, in equation (6c), can be written in terms of one of the fluctuation quadrature $X = (d + d^\dagger)/2$, in the following way: $4|\alpha|^2(\langle:X^2:\rangle - |\alpha|^2)$. If this is negative, there is some quadrature squeezing.

The four terms of this decomposition for $g_\sigma^{(2)}$ are shown in figure 2(a), as a function of the intensity of the driving laser. They always compensate exactly and the final result is, of course, the perfect sub-Poissonian statistics of the two-level system emission. However, as is clear in the figure, this compensation occurs in different ways depending on the driving regime [15]:

- In the region of large driving ($\Omega_\sigma \gg \gamma_\sigma$), where the spectrum of the emitter displays a Mollow triplet, we have that $\mathcal{I}_0 = -1$ with $\mathcal{I}_1 = \mathcal{I}_2 = 0$ meaning that antibunching appears solely due to the sub-Poissonian statistics of the fluctuations, that dominate over the vanishing coherent component $\lim_{\Omega_\sigma\to\infty}\alpha = 0$ (and therefore $d \to \sigma$).

- In the intermediate driving region ($\Omega_\sigma \sim \gamma_\sigma$), it is $\mathcal{I}_1 < 0$ that almost fully compensates the positive contributions of $1 + \mathcal{I}_0$. This is where $\mathcal{I}_0$ changes sign and the fluctuations become super-Poissonian.

- In the Heitler regime ($\Omega_\sigma \ll \gamma_\sigma$) that interests us more particularly, it is fluctuation squeezing that plays a major role, being this time the one responsible for antibunching, $\mathcal{I}_2 = -(1 + \mathcal{I}_0) = -2$.

Note that in the Heitler regime, $\mathcal{I}_1$ vanishes again. Consequently, resonance fluorescence reaches its maximum squeezing also in this region, an effect that has been confirmed in the emission from ensembles of atoms [74–78] and recently also from single atoms [79] and quantum dots [80]. Another way to understand the origin of antibunching in this region is as an interference between the coherent and incoherent parts of the emission (see equation (3)), since those terms which are either purely coherent (1) or purely incoherent ($\mathcal{I}_0$), are fully compensated by the 50%–50% mixed one, $\mathcal{I}_2$.

One can also compute the decomposition for the filtered second-order correlation function $g_a^{(2)}$ by applying again equations (6a)–(6c), now with the detector field operators, that is with $a \to \sigma$, $\langle n_\sigma\rangle \to \langle n_a\rangle$ and $\alpha = \langle a\rangle$. This is shown in figure 2(b) for the Heitler regime as a function of the filter width Γ. One can see how, with filtering, or equivalently when detection is taken into account, the terms no longer exactly compensate each other and their sum do not add up to exactly $g_a^{(2)} = 0$. Speaking in spectral terms, this is because the filter is leaving out some of the incoherent part that should compensate for the fixed coherent one (the delta function is always fully included in the convolution with the filter centred at $\omega_L = 0$). In the Heitler regime, this is clear when $\Gamma < \gamma_\sigma$, since γ_σ is the width of the (incoherent) Lorentzian peak, as shown in equation (3).

Figure 2. (a) Second-order correlation function of the emission from a two-level system (dashed black line) and its decomposition equation (5) into the four components (solid coloured lines) given by equations (6*a*)–(6*c*), as a function of the laser excitation. Regardless of the driving regime, the total emission fulfils $g_\sigma^{(2)} = 0$. In the Heitler regime, on the left-hand side, this is due to a destructive interference at the two-photon level between the coherent and incoherent (squeezed) components of resonance fluorescence. In the strong driving regime, right-hand side, perfect antibunching is due to the dominating sub-Poissonian fluctuations. (b) The same decomposition but now for the filtered emission $g_a^{(2)}$ and as a function of Γ in the Heitler regime ($\Omega_\sigma = 10^{-3}\,\gamma_\sigma$). In this case, the antibunching gets spoiled as the frequency resolution is increased by filtering, leading to an imperfect compensation of the components. This can however be restored with an external laser.

3. Destructive *N*-photon interference and antibunching restoration

The decomposition of the filtered second-order correlation function $g_a^{(2)}$ outlined above allows us to determine what is missing in terms of coherent and/or incoherent fractions to produce the perfect antibunching. Since the compensation comes, in part, from a coherent field, and such a field is easy to produce and control in the laboratory, one can actually *restore* full antibunching by superimposing to the filtered resonance fluorescence an external coherent field β, making them interfere at a beam splitter, and collecting the new signal for further use or analysis. We can find theoretically the value of β that ensures that the resulting total field, $s = t\,\sigma + r\,\beta$ (with t and r the transmission and reflection coefficients of the beam splitter, respectively, taken real and such that $r^2 + t^2 = 1$), although it has been filtered, still produces perfect antibunching at the output. We will call $\tilde{g}_a^{(2)}$ the second-order correlation function of this filtered signal that is interfered with a correcting external coherent beam, and proceed to show how to cancel it despite the filtering. This, in effect, realises the previously claimed subnatural-linewidth SPS [55, 56]. This becomes possible because the source is not a passive object anymore, that relates time and frequency of its emission merely through the Fourier transform, but includes a dynamical element. We will see in the following that, as a consequence, our source even achieves more than joint subnatural linewidth and antibunching.

The principle for antibunching restoration is simple. Since the filtering reduces the incoherent fraction, β should lower (proportionally) the coherent fraction. This is possible for two coherent fields by destructive interferences. That is, given that at resonance $\alpha = -i|\alpha|$, we should find a β of the form $\beta = i|\beta|$ such that the total mean field is reduced to $-i(t|\alpha| - r|\beta|)$. Out of resonance, both α and β have imaginary and real parts but the same idea would apply. This protocol and the condition for the external β-field are one of the chief results of this text. We now proceed to describe a possible setup to realise this interference and a theoretical model that provides an exact analytical condition.

The simplest and most reliable way to interfere resonance fluorescence with a controlled coherent field is to divert some light from the laser that excites the two-level system in the first place. In this way, one works with the same coherence time of the driving laser and should be immune to slow fluctuations. A possible setup is sketched in figure 1(a): the laser beam passes through a first beam splitter[4], that redirects part of it to the two-level system on one output arm and to an attenuator and a phase shifter on the other output arm. The emission of the two-level system (σ) and the attenuated laser (β) are admixed at a second beam splitter. The output constitutes our new antibunched source $s = t\sigma + r\beta$, which can be further analysed, measuring, for instance, its second-order correlation function in a Hanbury-Brown–Twiss setup, as depicted in the figure.

In the theoretical description, we include the detectors in the dynamics to now receive simultaneously the attenuated laser and the emission of the emitter $s = t\sigma + r\beta$. This is modelled by adding a coherent driving term to the detector $H_a = \mathrm{i}\Omega_a(a^\dagger - a)$, substituting $H \to H + H_a$ in equation (1), with $\Omega_a \in \mathbb{R}$. Note that the phase of the detector driving is fixed to $\beta = \mathrm{i}\Omega_a/g$ and the resulting Hamiltonian is then $H + H_a = \Omega_\sigma\sigma + g(t\sigma + \mathrm{i}r\Omega_a/g)a^\dagger + \text{h.c.}$ In this way, the detector is effectively performing the described homodyne procedure between the light emitted by the two-level system and a coherent field with amplitude $r\Omega_a/(tg)$. Furthermore, our model describes detection self-consistently and allows us to study the joint dynamical properties (in both time and frequency) of the light produced by the superposition. Since we are interested in the low driving limit, we express Ω_a in terms of Ω_σ through a new dimensionless parameter:

$$\mathcal{F} = \frac{r}{t}\frac{\gamma_\sigma\,\Omega_a}{g\,\Omega_\sigma}. \tag{7}$$

We also define $\mathcal{F}' = \mathcal{F}t/r$, which absorbs the dependence on the transmission and reflection parameters of the beam splitter. We take both $\mathcal{F}$ and $\mathcal{F}'$ to be real and positive. With these definitions, $\beta = \mathrm{i}\Omega_\sigma\mathcal{F}'/\gamma_\sigma$ and it is clear that $100\mathcal{F}'$ is then the percentage of the laser intensity that finally interferes with resonance fluorescence while $\mathcal{F}$ is the fraction that is needed to attenuate the laser for the compensation to be effective. The total mean field of the signal that exits the beam splitter towards detection (the right-hand side in figure 1(a)) reads $\langle s \rangle = t\alpha + r\beta = -\mathrm{i}\Omega_\sigma t(2 - \mathcal{F})/\gamma_\sigma$.

Next, we solve the new master equation in the Heitler regime, following the procedure in appendix A, we find that the detected Nth-order correlation function is

$$\tilde{g}_a^{(N)} = g_a^{(N)}\left[\frac{\sum_{k=0}^{N}\binom{N}{k}2^k(-\mathcal{F}')^{N-k}\prod_{\lambda=1}^{N-k}\left[1 + (N-\lambda)\Gamma/\gamma_\sigma\right]}{(2-\mathcal{F}')^N}\right]^2, \tag{8}$$

where $\tilde{g}_a^{(N)}$ is for the compensated signal and $g_a^{(N)}$ is given by equation (4). Note that all $\tilde{g}_a^{(N)}$ have a divergence at $\mathcal{F}' = 2$, independently of the filtering parameter Γ/γ_σ. This is another type of interference related to superbunching that lies beyond the scope of the present analysis and that is discussed elsewhere [81]. For $N = 2$ the correlation in equation (8) simplifies to

$$\tilde{g}_a^{(2)} = \left[\frac{4\gamma_\sigma - (4-\mathcal{F}')\mathcal{F}'(\gamma_\sigma + \Gamma)}{(2-\mathcal{F}')^2(\gamma_\sigma + \Gamma)}\right]^2, \tag{9}$$

which becomes exactly zero when the attenuation factor takes the two values

$$\mathcal{F}'_{2,\pm} = 2\left(1 \pm \sqrt{\frac{\Gamma}{\Gamma + \gamma_\sigma}}\right). \tag{10}$$

This result is valid to first (leading) order in Ω_σ, meaning that when the condition (10) is fulfilled, $\tilde{g}_a^{(2)} = 0$ with deviations due to higher-order terms in the driving only, so remaining extremely small. The antibunching becomes 'exactly zero' only in the limit of vanishing driving. In fact, would $\tilde{g}_a^{(2)}$ be exactly zero, then also all higher-order terms would satisfy $\tilde{g}_a^{(N)} = 0$ for $N \geqslant 2$ [82] and provide the ultimate, perfect SPS that emits a Fock state of a single photon, so with vanishing signal over time. In the Heitler regime but with a finite signal, the antibunching remains so small as to be well approximated by zero on the figures, in contrast to normal resonance fluorescence.

Note that the protocol we have just outlined becomes meaningless for two extreme cases: in the limit of broad filters, where we recover perfect antibunching without the interference, $\lim_{\Gamma\to\infty}\mathcal{F}'_{2,-} = 0$, and in the limit of vanishingly narrow filters, where $\lim_{\Gamma\to 0}\mathcal{F}'_{2,\pm} = 2$ and $\tilde{g}_a^{(N)}$ diverges. The latter case means that if the filter is very narrow, compensating for the loss of the incoherent component becomes impossible, as one ends up removing completely the coherent component with no signal left. One can nevertheless reduce the linewidth by

---

[4] We have not taken into account the first beam splitter of figure 1 in the calculations for simplicity, but, assuming it is balanced (50:50), doing so would simply rescale the original driving to $2\Omega_\sigma$ in order to obtain the results in the manuscript.
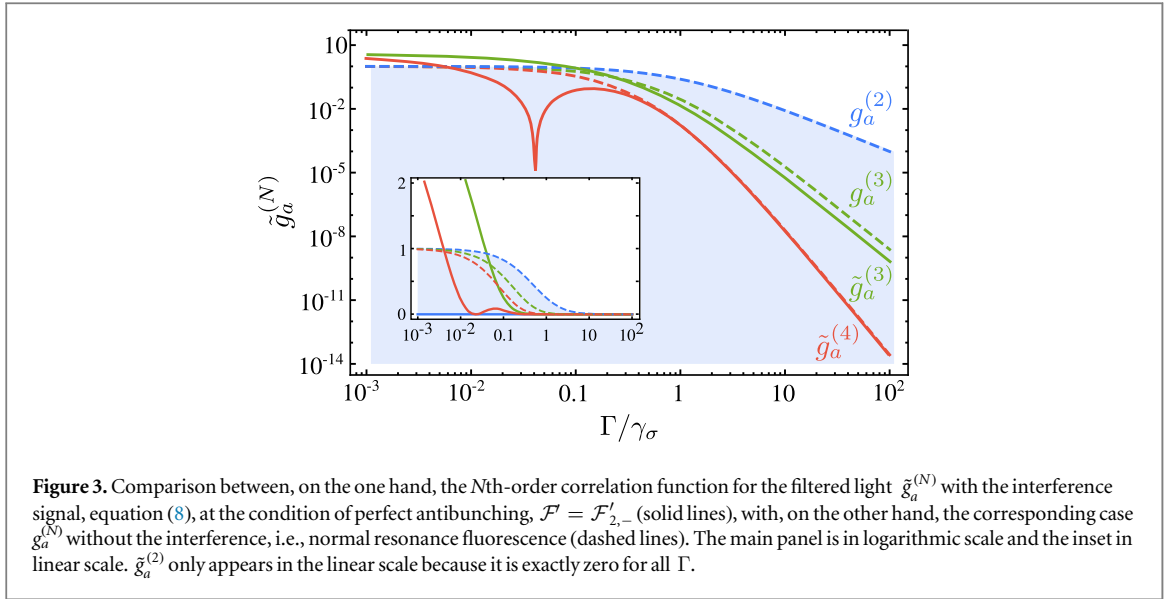
Figure 3. Comparison between, on the one hand, the *N*th-order correlation function for the filtered light $\tilde{g}_a^{(N)}$ with the interference signal, equation (8), at the condition of perfect antibunching, $\mathcal{F} = \mathcal{F}'_{2,-}$ (solid lines), with, on the other hand, the corresponding case $g_a^{(N)}$ without the interference, i.e., normal resonance fluorescence (dashed lines). The main panel is in logarithmic scale and the inset in linear scale. $\tilde{g}_a^{(2)}$ only appears in the linear scale because it is exactly zero for all Γ.

over an order of magnitude as compared to the natural linewidth of the emitter, which amply qualifies as a subnatural linewidth.

    The two solutions in equation (10) correspond to two different mean fields that, despite having different phases, lead to the same intensity in the interference signal, $\langle s_\pm \rangle = t\alpha + r\beta_\pm = \pm 2i\Omega_\sigma t/\gamma_\sigma \sqrt{\Gamma/(\Gamma + \gamma_\sigma)}$, and, therefore, both successfully compensate for the incoherent component, recovering perfect antibunching for any given realistic detection resolution Γ. Nevertheless, they are of a very different character: $\mathcal{F}'_{2,+}$ changes the phase of the original mean field, from $\alpha = -i|\alpha|$ to $\langle s_+ \rangle = i|t\alpha + r\beta_+|$, while $\mathcal{F}'_{2,-}$ corrects for the intensity maintaining the same phase $\langle s_- \rangle = -i|t\alpha + r\beta_-|$. This manifests in the higher-order correlation functions (8): while evaluating them at $\mathcal{F} = \mathcal{F}'_{2,+}$ does not lead to small values, for $\mathcal{F} = \mathcal{F}'_{2,-}$ they remain close to zero as well (although in general do not recover the exact zero)[5]. Note that, by performing a *wave-function expansion*, following the procedure in [83, 84], on the joint state of the emitter and detector, the attenuation fractions in equation (10) yield a suppression of the two-photon probability in the detector [81]. This corroborates the idea that perfect antibunching is recovered thanks to an interference effect at the two-photon level, that is, involving not only coherently scattered photons but also the incoherent (second order) ones in equation (3).

    In figure 3, we show the correlation functions for the interference signal, equation (8), when the condition for perfect antibunching is met, i.e., $\mathcal{F} = \mathcal{F}'_{2,-}$, so that $\tilde{g}_a^{(2)} = 0$ (solid lines), and we compare it to the case without the interference, i.e., $\mathcal{F} = 0$ (dashed lines), which is the case from the literature [55, 56]. We plot the cases $N = 2$ (blue), 3 (green) and 4 (red), as a function of the spectral width of the detector, Γ/γ_σ. Note that the solid blue line does not appear in the main figure which is in logarithmic scale, because its value is exactly zero to this order in the Heitler regime. This is the main result as compared to $g_a^{(2)}$ which, although it can get relatively small, can do so only for broad linewidths, and loses its antibunching for narrow lines. In stark contrast, the perfect antibunching for the interference signal remains satisfied even when the filter is much narrower than the natural linewidth of the emitter. On the other hand, the higher-order correlation functions also yield noteworthy results, which we will only briefly discuss. In contrast to $\tilde{g}_a^{(2)}$ which always remain much smaller than its unfiltered counterpart, there are filter linewidths where the interference results in larger higher-order correlations as compared to the standard case. This is clear in the inset of figure 3 which is in linear scale. If one wants to remain within small values of this higher-order functions, this limits how narrow the filtering can be, though still allowing for considerable improvement. We have also already noted how one is limited by the signal. Finally, even though perfect antibunching remains true for arbitrarily narrow filters in the theory, as $\Gamma \ll \gamma_\sigma$, the system would become unstable under possible small variations of the laser intensity: $\lim_{\Gamma \to 0} \mathcal{F}'_{2,-} = 2$, which is a diverging point for $\tilde{g}_a^{(2)}(\tau)$. A small fluctuation in the laser intensity would bring the system from perfect antibunching to a huge superbunching [81]. This could be seen as an advantage, providing a highly tunable quantum photon source that can be switched between antibunching and bunching by slightly adjusting

---

[5] For every N there are two values, $\mathcal{F}'_{N,\pm}$, that lead to $\tilde{g}_a^{(N)} = 0$, but they do not imply zero values for the other functions in general. Remarkably, for a given N and the parameter $\mathcal{F}'_{N,-}$, there is always a $\Gamma_{N,N'}$ for which also the coherence function N' is exactly zero, as long as $N' > N + 1$. Therefore, exact zeros are found for pairs of coherence functions, $\{N, N' > N + 1\}$, when using this particular pair of parameters $\{\mathcal{F}_{N,-}, \Gamma_{N,N'}\}$. For instance, $\Gamma_{2,4} = \gamma_\sigma/24$ and $\Gamma_{2,5} = (4 \pm \sqrt{13})\gamma_\sigma/12$. Since the antibunching obtained with our scheme is due to interference between coherent and incoherent components and there are only two parameters left in equation (9), it is reasonable that the condition $\tilde{g}_a^{(N)} = 0$ can be satisfied for two different N, N' simultaneously, obtaining two conditions for $\mathcal{F}$ and Γ.

the second laser attenuation. However, this superbunching effect also follows from an interference and is not linked to N-photon emission or other types of structured emission [81].

A representative filter linewidth for optimal operation can be taken as $\Gamma = \gamma_\sigma/5$, which we also use as the reference case in the following figures, because it is well below the natural emitter linewidth and brings an improvement essentially everywhere, i.e., we find that the interference yields the values $\tilde{g}_a^{(2)} = 0$, $\tilde{g}_a^{(3)} = 0.36$ and $\tilde{g}_a^{(4)} = 0.08$ while without the interference, one gets $g_a^{(2)} = 0.69$, $g_a^{(3)} = 0.35$ and $g_a^{(4)} = 0.14$. Note also the existence of a second local minimum for $\tilde{g}_a^{(4)}$ in figure 3. We find that there is such a local minimum for all higher-order correlators except the one that immediately follows the one that is exactly cancelled by the interference (i.e., $\tilde{g}_a^{(3)}$ in this case). Further discussion of the quantum state generated by this interference would lead us too far astray, therefore we now turn to two other quantities of considerable interest for single-photon emission purposes.
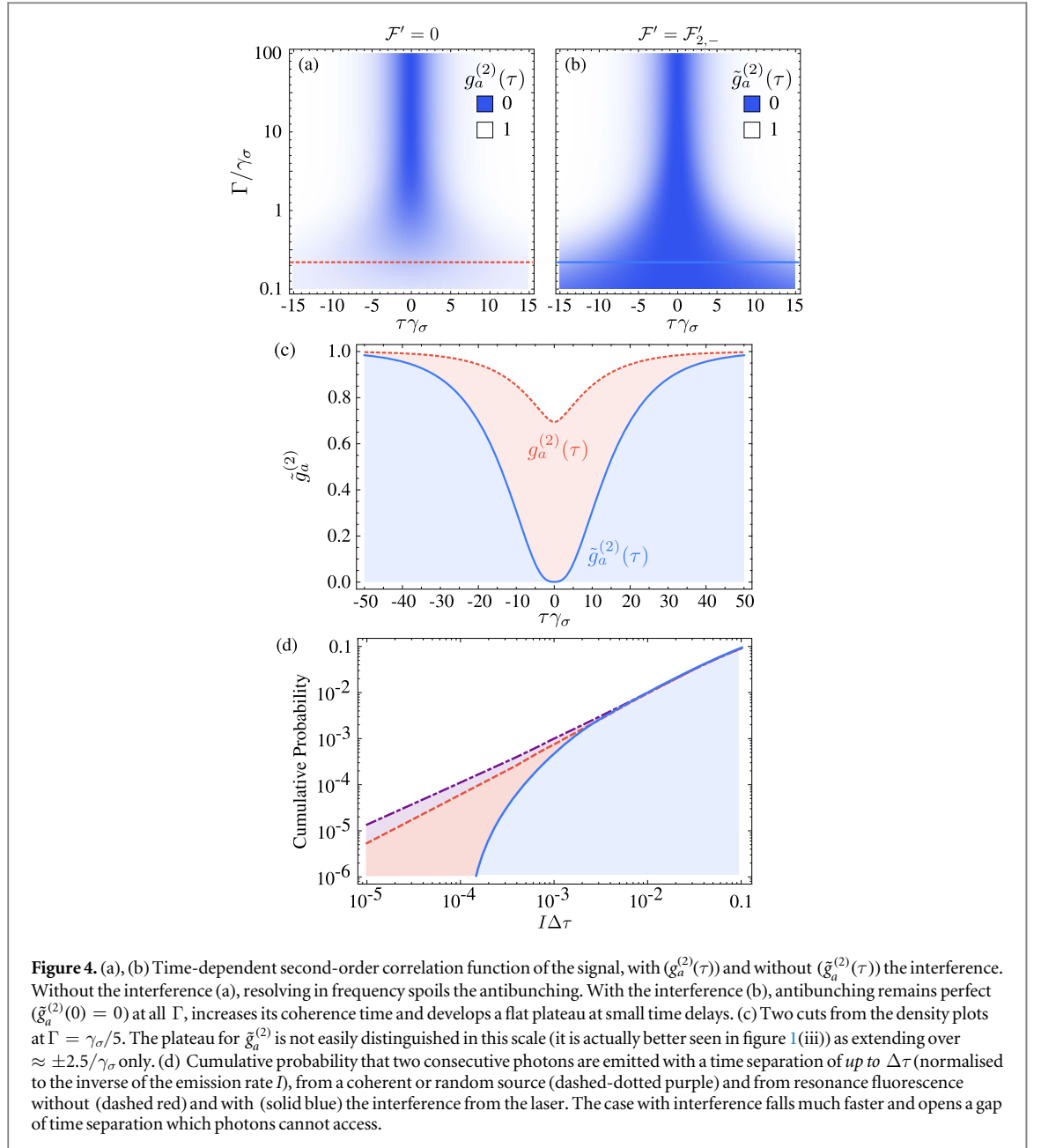
4. Coherence time and emission rate

So far, we have focused on two aspects of the SPS: its second-order correlation function at zero time delay, $\tilde{g}_a^{(2)}$ (which by abuse of language we occasionally refer to as 'antibunching'), and the spectral width of the emission, as it is observed or, equivalently, filtered, Γ. There are two other quantities which are of prime importance to characterise such a source: its coherence time, which estimates how long the correlations are retained, and the amount of signal. We now discuss them in turn, starting with the coherence time, which will show that the best features of the SPS remain to be presented.

In most SPSs, other than the one we present, the coherence time has to be longer than the temporal resolution of the detector, or the correlations become randomised. Also, they are required to evolve smoothly rather than featuring huge oscillations, that are sometimes observed in the wake of strong antibunching [85]. To characterise our source in this respect, we consider the time-resolved second-order correlation function $\tilde{g}_a^{(2)}(\tau)$, which can be computed from our master equation (1), deriving the equations from appendix A and applying the quantum regression theorem. Although in the following we present numerical results for these correlations, so as to easily access arbitrary time delays, the same procedure as for the zero-delay case can produce some closed-form but lengthy formulas in the Heitler regime, as is detailed in appendix A[6].

In figure 4, we compare the delayed second-order correlation function as measured by the detectors for (a) resonance fluorescence only, i.e., setting $\mathcal{F} = 0$, with (b) its interference with the optimally attenuated laser, i.e., $\mathcal{F} = \mathcal{F}'_{2,-}$, as previously discussed. For broad enough filters, when $\Gamma \gg \gamma_\sigma$, the measured correlations are perfectly antibunched and identical for both configurations. This happens because such wide filters collect the full spectrum and the interference occurs naturally. However, as the width of the filters becomes comparable to the natural linewidth of the emitter, the behaviour of the correlations in the two configurations start to differ. Without the interference with the attenuated laser, antibunching is rapidly lost (see dotted red line in figure 4(c)) and, in the limit $\Gamma \ll \gamma_\sigma$, the emission becomes completely randomised, with $\lim_{\Gamma \to 0} g_a^{(2)}(\tau) = 1$. However, with the interference, perfect antibunching is preserved regardless of the width of the filter, as already stated. Here, two new effects are remarkable: (i) the coherence time, or the time between single-photon emission, increases as the filter width becomes narrower and (ii) the correlations display a plateau of $\tilde{g}_a^{(2)}(\tau) = 0$ around $\tau = 0$. This plateau is particularly noteworthy. It is not entirely obvious on the scale of figure 4(c) since its extent is over $\tau\gamma_\sigma = \pm 2.5$ only, but it results in a dramatic type of correlations for the photons. Namely, such a plateau, as opposed to the standard case whose derivative is zero at zero-coincidences only, corresponds to opening a gap in the time separation between consecutive photons, meaning that while the case without interference makes it only very unlikely to find photon arbitrarily close, the interference SPS makes it impossible. In this sense, this restores a notion of 'perfect antibunching' even though the $\tilde{g}_a^{(2)}$ to all orders does not cancel exactly. The character of such correlations is better seen in figure 4(d), which shows the cumulative probability that a pair of *consecutive* photons are separated by a delay of up to $\Delta\tau$, as a function of this delay which, so as to compare photon sources with different emission rates, we have normalised to the mean delay between consecutive photons (which is given by the inverse of the emission rate, $1/I$). These results have been obtained with a quantum Monte Carlo simulation of the filtered resonance fluorescence [66]. We compare three cases: a coherent (random) source (dashed-dotted purple), and then the SPS without (dashed red) and with (solid blue) the interference from the laser. For delays larger than $I\Delta\tau \approx 10^{-2}$ the lines for the three sources converge, since at such large delays, the short-time correlations are lost and dominated by pure randomness, therefore recovering the uncorrelated case. At about $I\Delta\tau \approx 10^2$, the lines further saturate to unity, as they should from probability normalisation.

---

[6] $\tilde{g}_a^{(2)}(\tau)$ could be computed analytically in the case of simple detection of resonance fluorescence only, with $\mathcal{F} = 0$, using the formulas for the frequency and time-resolved correlation functions in the supplemental material of [64] and setting the detection frequency to zero.

Figure 4. (a), (b) Time-dependent second-order correlation function of the signal, with ($g_a^{(2)}(\tau)$) and without ($\tilde{g}_a^{(2)}(\tau)$) the interference. Without the interference (a), resolving in frequency spoils the antibunching. With the interference (b), antibunching remains perfect ($\tilde{g}_a^{(2)}(0) = 0$) at all Γ, increases its coherence time and develops a flat plateau at small time delays. (c) Two cuts from the density plots at $\Gamma = \gamma_\sigma/5$. The plateau for $\tilde{g}_a^{(2)}$ is not easily distinguished in this scale (it is actually better seen in figure 1(iii)) as extending over $\approx \pm 2.5/\gamma_\sigma$ only. (d) Cumulative probability that two consecutive photons are emitted with a time separation of *up to* $\Delta\tau$ (normalised to the inverse of the emission rate I), from a coherent or random source (dashed-dotted purple) and from resonance fluorescence without (dashed red) and with (solid blue) the interference from the laser. The case with interference falls much faster and opens a gap of time separation which photons cannot access.

The interesting features lie at short delays. There, it is seen that, while for the coherent source the cumulative probability increases linearly as $I\Delta\tau$ (the exact expression for this simple case being $1 - \exp(I\Delta\tau)$), for the emitter without the interference, the growth is slower because of its antibunching, which lowers the probability for photons to be detected close to each other. The difference is however small and the trend is qualitatively similar to that of the uncorrelated photon source! Indeed, such a difference is eclipsed by the type of suppression that is observed by the emitter with the interference (solid blue line). There, the departure is much more pronounced and is qualitatively of a different character, increasing its slope till a point where it would become vertical, meaning the complete impossibility to ever detect two photons closer to each other than a finite nonzero time window. This suppression comes from the plateau in the $\tilde{g}_a^{(2)}(\tau)$, and shows how the enhancement in the correlations that is obtain through the interference cannot be obtained by using another emitter operating in a different timescale.

As a final important characteristic, we have to address the only feature for which our proposed SPS does not overcome the other types of sources: the intensity of the signal. One of the acclaimed qualities of resonance fluorescence is that it is ultrabright [55, 56], being indeed efficiently excited by a resonant laser, in the first place. Note that an incoherently driven SPS would be brighter still as it can saturate the emitter, providing twice as much signal than under coherent driving which is limited by stimulated emission. The incoherently pumped SPS would, however, emit photons of completely undetermined frequency due to power broadening. In our case, the whole procedure comes at the price of losing signal, i.e., of reducing the total emission rate $I = \Gamma\langle n_a \rangle$.

This is done in two ways: by filtering out the incoherent fraction or resonance fluorescence to narrow its lineshape (which technically should also toll other systems claiming subnatural linewidths) but also, in order to compensate this loss of the incoherent fraction, by removing part of the coherent fraction through destructive interferences with the laser. The total emission will thus clearly be reduced. To evaluate the brightness of our homodyne scheme I_{int}, let us first obtain that of filtered resonance fluorescence $I_{\text{r.f.}}$. The population of the detector $\langle n_a \rangle$ is related to the population of the emitter that feeds it, $\langle n_\sigma \rangle$, through the emission spectrum at resonance $S_{\Gamma,\sigma}(\omega = 0)$ by

$$\langle n_a \rangle = \frac{|g|^2}{\Gamma} 2\pi \langle n_\sigma \rangle S_{\Gamma,\sigma}(\omega = 0), \tag{11}$$

(see the equivalences in the supplemental of [64]), as long as there is no extra driving of the detector. Considering the correspondence between the sensor method [64] and the cascaded formalism (see [66]), we can write $|g| \to \sqrt{\Gamma \gamma_\sigma}$. We substitute as well the spectrum convoluted with the detector, as explained in equation (B.9) of the appendix B, which in the Heitler regime is simply

$$S_{\Gamma,\sigma}(\omega) = \frac{1}{\pi} \frac{\Gamma/2}{(\Gamma/2)^2 + \omega^2}. \tag{12}$$

Since we are interested in the rates to first order in the driving Ω_σ, only coherently scattered photons (the first term in equation (3)) are included in this derivation. The emission rate from the filtered resonance fluorescence then converges to the original emission (without detection):

$$I_{\text{r.f.}} = \gamma_\sigma \langle n_\sigma \rangle = 4\Omega_\sigma^2 / \gamma_\sigma. \tag{13}$$

In the case of interference with the attenuated laser, the spectrum of emission remains the same (the coherent part only, to first order in Ω_σ) but the population is now that of the total admixed signal:

$$I_{\text{int}} = \gamma_\sigma \langle n_s \rangle. \tag{14}$$

This population can be easily computed:

$$\langle n_s \rangle = t^2 \langle n_\sigma \rangle + r^2 |\beta|^2 + 2rt\,\Re[\langle \sigma \rangle \beta^*] = t^2 \left(1 - \frac{\mathcal{F}}{2}\right)^2 \frac{4\Omega_\sigma^2}{\gamma_\sigma^2}. \tag{15}$$

Finally, by comparing equation (13) with (14) and (15), we find that the interference with the laser reduces the emission rate by a factor related to $\mathcal{F}$, as

$$\frac{I_{\text{int}}}{I_{\text{r.f.}}} = t^2 (1 - \mathcal{F}/2)^2. \tag{16}$$

For the condition that yields perfect antibunching ($\mathcal{F} = \mathcal{F}_{2,-}$), this reduces to

$$\frac{I_{\text{int}}}{I_{\text{r.f.}}} = t^2 \frac{\Gamma}{\Gamma + \gamma_\sigma}. \tag{17}$$

The signal is reduced from the filtering procedure by a factor $\Gamma/(\Gamma + \gamma_\sigma)$, times the loss of the beam splitter by a factor t^2. This last factor could be overcome by using an unbalanced beam splitter where $t \sim 1$ and attenuating the laser accordingly. Still, the brightness is reasonably good, for instance, for our reference case, $\Gamma = \gamma_\sigma/5$, the reduction is only of a factor $I_{\text{int}}/I_{\text{r.f.}} = 1/6$. On the other hand, we have gained enormously in antibunching and the linewidth is narrow indeed.

In figure 5 we can see the comparison between both cases in a parametric plot where Γ is varied, with the width of the filters being encoded in the colour gradient of each line, starting from black in the limit of $\Gamma \to \infty$, and ending with the respective colours, in the limit of $\Gamma \to 0$. The dashed red line corresponds to the case of filtered resonance fluorescence but without interference. Its emission rate remains constant regardless of the filter width following equation (13), with still most of the emission being provided by the delta peak anyway. However, $g_a^{(2)}$ is quickly lost, as was previously discussed. The solid blue line shows the case with interference, and $\tilde{g}_a^{(2)}$ there remains at zero independently of the filter width, but at the cost of lowering its emission rate, in agreement with equation (14).

We compare them with a third case to evidence again that in presence of the interference, the emitter turns into a qualitatively different type of SPS. Indeed, one could argue that the problem of finding a bright monochromatic source with perfect antibunching for a given detector, could be solved simply by using an emitter with a linewidth $\hat{\gamma}_\sigma$ smaller than that of the detector, $\hat{\gamma}_\sigma \ll \Gamma < \gamma_\sigma$, so that, by keeping the same driving intensity, the emitter can be excited more efficiently. For the comparison to be fair, the choice of $\hat{\gamma}_\sigma$ would have to be done in such a way that the properties of the emitted light are equal to the ones obtained with our scheme, namely: the emission spectrum and the coherence time of the $\tilde{g}_a^{(2)}(\tau)$ have to be comparable in both cases. This results in the dashed-green line where, for each filter size Γ, we choose an emitter with linewidth $\hat{\gamma}_\sigma < \gamma_\sigma$ such that the emission spectra and the coherence time are equal to those obtained with our scheme. With this
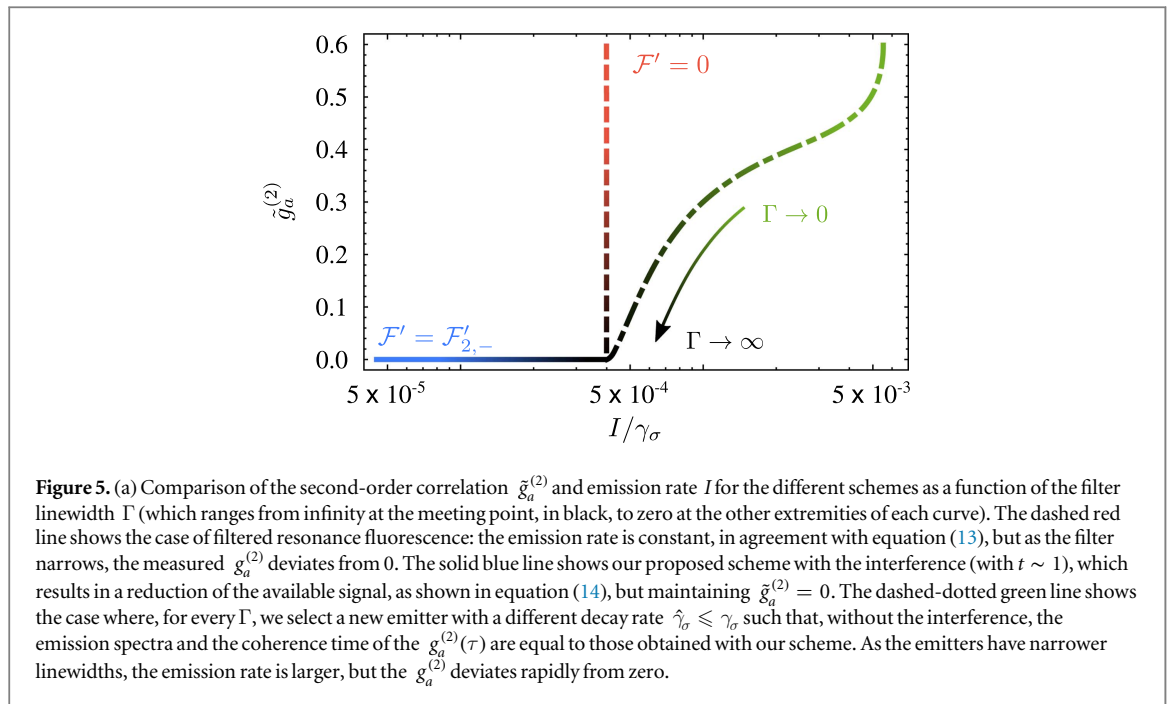
Figure 5. (a) Comparison of the second-order correlation $\tilde{g}_a^{(2)}$ and emission rate I for the different schemes as a function of the filter linewidth Γ (which ranges from infinity at the meeting point, in black, to zero at the other extremities of each curve). The dashed red line shows the case of filtered resonance fluorescence: the emission rate is constant, in agreement with equation (13), but as the filter narrows, the measured $g_a^{(2)}$ deviates from 0. The solid blue line shows our proposed scheme with the interference (with $t \sim 1$), which results in a reduction of the available signal, as shown in equation (14), but maintaining $\tilde{g}_a^{(2)} = 0$. The dashed-dotted green line shows the case where, for every Γ, we select a new emitter with a different decay rate $\hat{\gamma}_\sigma \leqslant \gamma_\sigma$ such that, without the interference, the emission spectra and the coherence time of the $g_a^{(2)}(\tau)$ are equal to those obtained with our scheme. As the emitters have narrower linewidths, the emission rate is larger, but the $g_a^{(2)}$ deviates rapidly from zero.

configuration, the emission rate becomes larger with broader linewidths (because the emitter with linewidth $\hat{\gamma}_\sigma$ gets excited more easily than the one with linewidth γ_σ), but such an enhancement in the emission rate comes at the price of an increase in the zero-delay $g_a^{(2)}$, as seen in the figure. There, it is clear that all the sources have a point in common, which is the case when all frequencies are detected. Imposing some frequency resolution results in some departures. It appears obvious in the light of the demands made by a quantum circuit that the only one truly tolerable for quantum applications are those suffered by our SPS.

We conclude with a quick overview of the feasibility of the proposed setup. This type of interference between the original signal and a controlled laser beam (or *local oscillator*) is a standard technique in quantum optics, known as *homodyne measurement* [71–73, 86–96]. In particular, looking at the second-order correlation function when tuning the laser beam properties was first suggested by Vogel [72, 73], to analyse the squeezing properties of the signal. Several recent works [94, 95, 97] have also used this concept with a different objective, namely, to subtract the coherent fraction from the signal (in their case the emission from a cavity in strong coupling with a quantum dot). Thanks to this procedure, they could observe the strong quantum features of the remaining incoherent fraction such as increased indistinguishability, antibunching or a pulsed Mollow triplet spectrum. Our analysis, focused on the fundamental mechanism, did not include the complications present in some of the promising platforms to implement the effect, such as quantum dots. There, impact of dephasing for instance should be taken into account and we have done this in a follow-up work [98]. Still other details, like the fine-structure splitting, could also be included in increasingly more refined studies. On the basis of the physical principle that allows the effect to take place, however, we see no *a priori* reason why it could not fully apply also in more complex structures, at the price of possibly heavier expressions for the resonant condition and more intricate experimental configurations. It seems therefore clear to us that the variations needed to implement our scheme are definitely within reach of the existing setups and that one could thus, in this way, finally realise a source with rapidly vanishing second-order correlation function and subnatural linewidth, simultaneously.

5. Conclusions

In conclusion, we have shown how to implement a new type of SPS that outperforms what is currently available on every account except in terms of the available signal. This is based on a variation of resonance fluorescence in the Heitler regime, which has been claimed in the literature to provide very good antibunching as well as spectrally narrow emission. We have shown how such properties in fact do not coexist in resonance fluorescence in its bare form, due to neglecting the detection process of the emitted light, that needs to consider jointly these two properties.

However, it is possible to reach this regime, by compensating for the loss of antibunching caused by the spectral resolution of the detector, or, equivalently, by filtering. By decomposing the second-order correlation function into various types of field fluctuations, we have shown how one component, the coherent one, can easily be corrected externally to restore the balance which yields perfect antibunching (to first order in the

driving). We provided an analytical expression for the condition to fulfil and proposed a setup to implement this scheme. We find that the light that is produced indeed provides subnatural linewidth and vanishing antibunching, at the only cost of a diminished signal, which remains, however, less than a factor of magnitude drop for reasonable parameters. Interestingly, the photon correlations in time exhibit a new qualitative trend, in the form of a plateau, which results in a time window where photon coincidences are suppressed exactly. This leads to the realisation of a perfect SPS, in the sense that a superconductor is a perfect conductor: our source will never produce a coincidence in an Hanbury-Brown–Twiss setup whose correlation time is smaller than this plateau. This is true to first order in the driving, meaning than in an actual setup, the waiting time to observe such a coincidence will not be infinite, but only as large as required, which is not possible with a conventional SPS.

Acknowledgements

Appendix A. Steady state of the combined resonance fluorescence and detector at vanishing laser driving

We first solve the dynamics for the mean value of any system operator, which in its most general normally ordered form reads [99] $C_{\{m,n,\mu,\nu\}} = \langle \sigma^{\dagger m} \sigma^n a^{\dagger \mu} a^\nu \rangle$ (with $m, n \in \{0,1\}$ and $\mu, \nu \in \mathbb{N}$). It follows the equation:

$$\partial_t C_{\{m,n,\mu,\nu\}} = \sum_{m',n',\mu',\nu'} \mathcal{M}^{m,n,\mu,\nu}_{m',n',\mu',\nu'} C_{\{m',n',\mu',\nu'\}}, \tag{A.1}$$

with the regression matrix elements $\mathcal{M}^{m,n,\mu,\nu}_{m',n',\mu',\nu'}$ given by, in our case:

$$\mathcal{M}^{m,n,\mu,\nu}_{m,n,\mu,\nu} = -\frac{\gamma_\sigma}{2}(m+n) - \frac{\Gamma}{2}(\mu+\nu), \qquad \mathcal{M}^{m,n,\mu,\nu}_{m,1-n,\mu,\nu} = -i\Omega_\sigma[n + 2m(1-n)], \tag{A.2}$$

$$\mathcal{M}^{m,n,\mu,\nu}_{1-m,n,\mu,\nu} = i\Omega_\sigma[m + 2n(1-m)], \qquad \mathcal{M}^{m,n,\mu,\nu}_{m,n,\mu,\nu-1} = \Omega_a \nu, \tag{A.3}$$

$$\mathcal{M}^{m,n,\mu,\nu}_{m,n,\mu-1,\nu} = \Omega_a \mu, \qquad \mathcal{M}^{m,n,\mu,\nu}_{1-m,n,\mu-1,\nu} = -g(1-m)\mu, \tag{A.4}$$

$$\mathcal{M}^{m,n,\mu,\nu}_{m,1-n,\mu,\nu-1} = -g(1-n)\nu \tag{A.5}$$

and zero everywhere else. These equations can be solved numerically, choosing a high enough truncation in the number of photons, in order to obtain a converged steady state ($\partial_t C_{\{m,n,\mu,\nu\}} = 0$) for any given pump power. However, it is possible to derive analytical solutions in the case where we use a 'sensor' ($g \to 0$) in the vanishing driving limit ($\Omega_\sigma \to 0$ after setting $\Omega_a = g\Omega_\sigma \mathcal{F}/\gamma_\sigma$). In this case, it is enough to solve recursively sets of truncated equations. That is, we start with the lowest order correlators, with only one operator, which we write in a vectorial form for convenience: $\mathbf{v}_1 = (\langle a \rangle, \langle a^\dagger \rangle, \langle \sigma \rangle, \langle \sigma^\dagger \rangle)^\mathrm{T}$. Its equation reads $\partial_t \mathbf{v}_1 = M_1 \mathbf{v}_1 + A_1 + o(\Omega, g)$ where $o(\Omega, t)$ means higher-order terms of these variables, where Ω stands for both Ω_a and Ω_σ. This provides the steady state value $\mathbf{v}_1 = -M_1^{-1} A_1 + o(\Omega, g)$. We proceed in the same way with the two-operator correlators $\mathbf{v}_2 = (\langle a^2 \rangle, \langle a^{\dagger 2} \rangle, \langle a^\dagger a \rangle, \langle \sigma^\dagger \sigma \rangle, \langle \sigma^\dagger a \rangle, \cdots)^\mathrm{T}$, only, in this case, we also need to include the steady state value for the one-operator correlators as part of the independent term in the equation: $\partial_t \mathbf{v}_2 = M_2 \mathbf{v}_2 + A_2 + X_{21}\mathbf{v}_1 + o(\Omega, t)$. The steady state reads $\mathbf{v}_2 = -M_2^{-1}(A_2 + X_{21}\mathbf{v}_1) + o(\Omega, g)$ with a straightforward generalisation $\mathbf{v}_N = -M_N^{-1}(A_N + \sum_{j=1}^{N-1} X_{Nj}\mathbf{v}_j) + o(\Omega, g)$.

We are interested in this text in photon correlators of the form $\langle a^{\dagger N} a^N \rangle$. These follow $\langle a^{\dagger N} a^N \rangle \sim (\Omega_\sigma g)^{2N}$, to lowest order in both Ω_σ and g. The normalised correlation functions $g_\Gamma^{(N)}$ are thus independent of both Ω_σ and g to lowest order, and their computation requires to solve the $2N$ sets of recurrent equations and taking the limits $\lim_{g \to 0} \lim_{\Omega_\sigma \to 0} \langle a^{\dagger N} a^N \rangle / \langle a^\dagger a \rangle^N$. This can be done analytically and this provides equations (4) and (8) from the main text.

Appendix B. Two-time correlators and spectrum of emission for resonance fluorescence (at any laser driving, without detector)

First, using again the regression matrix (A.2)–(A.5), we write the equations (A.1) in a vectorial form for the two-level system only, by setting $g = 0$. In this case, one-time correlators follow $\partial_\tau \mathbf{w}[1, 1](\tau) = M_\sigma \mathbf{w}[1, 1](\tau) + A_\sigma$ with

$$\mathbf{w}[1,1](\tau) = \begin{pmatrix} \langle\sigma\rangle(\tau) \\ \langle\sigma^\dagger\rangle(\tau) \\ \langle\sigma^\dagger\sigma\rangle(\tau) \end{pmatrix}, \quad A_\sigma = i\Omega_\sigma \begin{pmatrix} -1 \\ 1 \\ 0 \end{pmatrix}, \quad M_\sigma = \begin{pmatrix} -\dfrac{\gamma_\sigma}{2} & 0 & 2i\Omega_\sigma \\ 0 & -\dfrac{\gamma_\sigma}{2} & -2i\Omega_\sigma \\ i\Omega_\sigma & -i\Omega_\sigma & -\gamma_\sigma \end{pmatrix}. \tag{B.1}$$

The steady state solution reads

$$\mathbf{w}[1,1] = \begin{pmatrix} \langle\sigma\rangle \\ \langle\sigma^\dagger\rangle \\ \langle\sigma^\dagger\sigma\rangle \end{pmatrix} = -M_\sigma^{-1} A_\sigma = \frac{2\Omega_\sigma}{\gamma_\sigma^2 + 8\Omega_\sigma^2} \begin{pmatrix} -i\gamma_\sigma \\ i\gamma_\sigma \\ \Omega_\sigma \end{pmatrix}. \tag{B.2}$$

By applying the quantum regression theorem which states that two-time correlators follow the same equations for the time delay as the single-time ones for time, we have that $\partial_\tau \mathbf{w}[L, R](\tau) = M_\sigma \mathbf{w}[L, R](\tau) + A_\sigma \langle LR\rangle$ for any two operators L, R, with

$$\mathbf{w}[L, R](\tau) = \begin{pmatrix} \langle L\,\sigma(\tau)R\rangle \\ \langle L\,\sigma^\dagger(\tau)R\rangle \\ \langle L(\sigma^\dagger\sigma)(\tau)R\rangle \end{pmatrix} \tag{B.3}$$

and $\mathbf{w}[L, R](0)$ obtained from the single-time mean values in $\mathbf{w}[1,1]$. The solution is given by:

$$\begin{aligned}
\mathbf{w}[L, R](\tau) &= e^{M_\sigma\tau}\{\mathbf{w}[L, R](0) + M_\sigma^{-1}A_\sigma\langle LR\rangle\} - M_\sigma^{-1}A_\sigma\langle LR\rangle \\
&= e^{M_\sigma\tau}\{\mathbf{w}[L, R](0) - \mathbf{w}[1, 1]\langle LR\rangle\} + \mathbf{w}[1, 1]\langle LR\rangle.
\end{aligned} \tag{B.4}$$

We compute the correlators that we need below and in the main text, by solving only two of these two-time correlator vectors, for $\mathbf{w}[\sigma^\dagger, \sigma](\tau)$ and $\mathbf{w}[1, \sigma](\tau)$, since we have

$$\langle\sigma^\dagger(\sigma^\dagger\sigma)(\tau)\sigma\rangle = \mathbf{w}[\sigma^\dagger, \sigma]_3(\tau), \quad \langle\sigma^\dagger\sigma^\dagger(\tau)\sigma\rangle = \mathbf{w}[\sigma^\dagger, \sigma]_2(\tau),$$
$$\langle(\sigma^\dagger\sigma)(\tau)\sigma\rangle = \mathbf{w}[1, \sigma]_3(\tau), \quad \langle\sigma^\dagger(\tau)\sigma\rangle = \langle\sigma^\dagger\sigma(\tau)\rangle^* = \mathbf{w}[1, \sigma]_2(\tau),$$
$$\langle\sigma^\dagger\sigma^\dagger(\tau)\rangle = \langle\sigma(\tau)\sigma\rangle^* = \{\mathbf{w}[1, \sigma]_1(\tau)\}^*.$$

The initial conditions read

$$\mathbf{w}[\sigma^\dagger, \sigma](0) = \begin{pmatrix} 0 \\ 0 \\ 0 \end{pmatrix} \quad \text{and} \quad \mathbf{w}[1, \sigma](0) = \begin{pmatrix} 0 \\ \langle\sigma^\dagger\sigma\rangle \\ 0 \end{pmatrix}. \tag{B.6}$$

We can thus provide the expression for the second-order correlation function of resonance fluorescence with perfect time resolution (or without coupling to a detector):

$$g_\sigma^{(2)}(\tau) = 1 - \left[\frac{3\gamma_\sigma}{4R_\sigma}\sinh(R_\sigma\tau) + \cosh(R_\sigma\tau) \right] e^{-3\gamma_\sigma\tau/4}, \tag{B.7}$$

in terms of $R_\sigma = \sqrt{(\gamma_\sigma/4)^2 - (2\Omega_\sigma)^2}$. Note that $\lim_{\Omega_\sigma \to 0} R_\sigma = \gamma_\sigma/4$ and that oscillations only appear in $g_\sigma^{(2)}(\tau)$ when $\Omega_\sigma > \gamma_\sigma/8$, as the two-level system enters into strong coupling with the laser.

On the other hand, the normalised steady state spectrum of emission with perfect frequency resolution [2, 68], is defined as

$$S_\sigma(\omega) = \frac{1}{\pi\langle n_\sigma\rangle}\Re\int_0^\infty \langle\sigma^\dagger\sigma(\tau)\rangle e^{i\omega\tau}d\tau. \tag{B.8}$$

Substituting the expression found for the correlator $\langle\sigma^\dagger\sigma(\tau)\rangle$ in equation (B.5) and expanding up to second order in the driving Ω_σ, we obtain the formula (3) in the main text.

The expression after convolution with a detector with spectral resolution Γ is:

$$S_{\Gamma,\sigma}(\omega) = \frac{1}{\pi\langle n_\sigma\rangle}\Re\int_0^\infty \langle\sigma^\dagger\sigma(\tau)\rangle e^{(i\omega-\Gamma/2)\tau}d\tau, \tag{B.9}$$

which is used to obtain equation (12).

ORCID iDs

J C López Carreño ● https://orcid.org/0000-0002-2134-0958
E Zubizarreta Casalengua ● https://orcid.org/0000-0003-4967-595X
F P Laussy ● https://orcid.org/0000-0002-1070-7128
E del Valle ● https://orcid.org/0000-0002-0221-282X

References

[1] Heitler W 1944 *The Quantum Theory of Radiation* (Oxford: Oxford University Press)
[2] Mollow B R 1969 *Phys. Rev.* **188** 1969
[3] Wu F Y, Grove R E and Ezekiel S 1975 *Phys. Rev. Lett.* **35** 1426
[4] Agarwal G S 1976 *Phys. Rev. Lett.* **37** 1383
[5] Kimble H J and Mandel L 1976 *Phys. Rev. A* **13** 2123
[6] Cohen-Tannoudji C N and Reynaud S 1977 *J. Phys. B.: At. Mol. Phys.* **10** 345
[7] Groove R E, Wu F Y and Ezekial S 1977 *Phys. Rev. A* **16** 227
[8] Kimble H J, Dagenais M and Mandel L 1977 *Phys. Rev. Lett.* **39** 691
[9] Dagenais M and Mandel L 1978 *Phys. Rev. A* **18** 2217
[10] Knight P L, Molander W A and C R Stroud J 1978 *Phys. Rev. A* **17** 1547
[11] Apanasevich P A and Kilin S Y 1979 *J. Phys. B.: At. Mol. Phys.* **12** L83
[12] Cohen-Tannoudji C and Reynaud S 1979 *Phil. Trans. R. Soc. A* **293** 223
[13] Mandel L 1979 *Opt. Lett.* **4** 205
[14] Singh S 1983 *Opt. Commun.* **44** 254
[15] Carmichael H J 1985 *Phys. Rev. Lett.* **55** 2790
[16] Kozlovskii A and Oraevskii A 1999 *J. Exp. Theor. Phys.* **88** 666
[17] Astafiev O, Zagoskin A M, Jr A A A, Pashkin Y A, Yamamoto T, Inomata K, Nakamura Y and Tsai J S 2010 *Science* **327** 840
[18] Verma V B, Stevens M J, Silverman K L, Dias N L, Garg A, Coleman J J and Mirin R P 2011 *Opt. Express* **19** 4182
[19] Berquist W M I J C and Wineland D J 1988 *Phys. Rev. A* **38** 559
[20] Grangier P, Roger G, Aspect A, Heidmann A and Reynaud S 1986 *Phys. Rev. Lett.* **67** 687
[21] Rempe G, Schmidt-Kaler F and Walther H 1990 *Phys. Rev. Lett.* **64** 2783
[22] Diedrich F and Walther H 1987 *Phys. Rev. Lett.* **58** 203
[23] Bergquist J C, Hulet R G, Itano W M and Wineland D J 1986 *Phys. Rev. Lett.* **57** 1699
[24] Schubert M, Siemers I, Blatt R, Neuhauser W and Toschek P E 1992 *Phys. Rev. Lett.* **68** 3016
[25] Kask P, Piksarv P and Mets U 1985 *Eur. Biophys. J.* **12** 163
[26] Basché T, Moerner W E, Orrit M and Talon H 1992 *Phys. Rev. Lett.* **69** 1516
[27] Treussart F, Clouqueur A, Grossman C and Roch J F 2001 *Opt. Lett.* **26** 1504
[28] Lounis B and Moerner W E 2000 *Nature* **407** 491
[29] Michler P, Kiraz A, Becher C, Schoenfeld W V, Petroff P M, Zhang L, Hu E and Imamoglu A 2000 *Science* **290** 2282
[30] Lounis B, Bechtel H A, Gerion D and Moerner P A W E 2000 *Chem. Phys. Lett.* **329** 399
[31] Santori C, Pelton M, Solomon G, Dale Y and Yamamoto Y 2001 *Phys. Rev. Lett.* **86** 1502
[32] Zwiller V, Blom H, Jonsson P, Panev N, Jeppessen S, Tsegaye T, Goobar E, Pistol M E, Samuelson L and Björk G 2001 *Appl. Phys. Lett.* **78** 2476
[33] Sebald K, Michler P, Passow T, Hommel D, Bacher G and Forshel A 2002 *Appl. Phys. Lett.* **81** 2920
[34] Santori C, Fattal D, Vuckovic J, Solomon G S and Yamamoto Y 2002 *Nature* **419** 594
[35] Pelton M, Santori C, Vučković J, Zhang B, Solomon G, Plant J and Yamamoto Y 2002 *Phys. Rev. Lett.* **89** 2333602
[36] Yuan Z, Kardynal B E, Stevenson R M, Shields A J, Lobo C J, Cooper K, Beattie N S, Ritchie D A and Pepper M 2002 *Science* **295** 102
[37] Gerardot B D, Strauf S, de Dood M J A, Bychkov A M, Badolato A, Hennessy K, Hu E L, Bouwmeester D and Petroff P M 2005 *Phys. Rev. Lett.* **95** 137403
[38] Bozyigit D *et al* 2011 *Nat. Phys.* **7** 154
[39] Lang C, Eichler C, Steffen L, Fink J M, Woolley M J, Blais A and Wallraff A 2013 *Nat. Phys.* **9** 345
[40] Hoi I, Wilson C M, Johansson G, Lindkvist J, Peropadre B, Palomaki T and Delsing P 2013 *New J. Phys.* **15** 025011
[41] Gu X, Kochum A F, Miranowicz C, Liu Y X and Nori F 2017 *Phys. Rep.* **718** 1
[42] Kurtsiefer C, Mayer S, Zarda P and Weinfurter H 2000 *Phys. Rev. Lett.* **85** 290
[43] Brouri R, Beveratos A, Poizat J P and Grangier P 2000 *Opt. Lett.* **25** 1294
[44] Messin G, Hermier J P, Giacobino E, Desbiolles P and Dahan M 2001 *Opt. Lett.* **23** 1891
[45] Kuhlmann A V, Prechtel J H, Houel J, Ludwig A, Reuter D, Wieck A D and Warburton R J 2015 *Nat. Commun.* **6** 8204
[46] Somaschi N *et al* 2016 *Nat. Photon.* **10** 340
[47] Ding X *et al* 2016 *Phys. Rev. Lett.* **116** 020401
[48] Wang H *et al* 2016 *Phys. Rev. Lett.* **116** 213601
[49] Kim J H, Cai T, Richardson C J K, Leavitt R P and Waks E 2016 *Optica* **3** 577
[50] Daveau R S *et al* 2017 *Optica* **4** 178
[51] Grange T, Somaschi N, Antón C, Santis L D, Coppola G, Giesz V, Lemaître A, Sanges I, Auffèves A and Senellart P 2017 *Phys. Rev. Lett.* **118** 253602
[52] Gibbs H M and Venkatesan T N C 1976 *Opt. Commun.* **17** 87
[53] Hartig W, Rasmussen W, Schieder R and Walther H 1976 *Z. Phys.* **278** 205
[54] Höffges J T, Baldauf H W, Eichler T, Helmfrid S R and Walther H 1997 *Opt. Commun.* **133** 170
[55] Nguyen H S, Sallen G, Voisin C, Roussignol P, Diederichs C and Cassabois G 2011 *Appl. Phys. Lett.* **99** 261904
[56] Matthiesen C, Vamivakas A N and Atatüre M 2012 *Phys. Rev. Lett.* **108** 093602
[57] Unsleber S, He Y M, Gerhardt S, Maier S, Lu C Y, Pan J W, Gregersen N, Kamp M, Schneider C and Höfling S 2016 *Opt. Express* **24** 8539
[58] Loredo J C *et al* 2016 *Optica* **3** 433
[59] He Y M, Liu J, Maier S, Emmerling M, Gerhardt S, Davanço M, Schneider C and Höfling S 2017 *Optica* **4** 802
[60] González-Tudela A, Laussy F P, Tejedor C, Hartmann M J and del Valle E 2013 *New J. Phys.* **15** 033036
[61] Eberly J and Wódkiewicz K 1977 *J. Opt. Soc. Am.* **67** 1252
[62] Knöll L and Weber G 1986 *J. Phys. B.: At. Mol. Phys.* **19** 2817
[63] Knöll L, Vogel W and Welsch D G 1990 *Phys. Rev. A* **42** 503
[64] del Valle E, González-Tudela A, Laussy F P, Tejedor C and Hartmann M J 2012 *Phys. Rev. Lett.* **109** 183601
[65] Gardiner G W and Zoller P 2000 *Quantum Noise* 2nd edn (Berlin: Springer)
[66] López Carreño J C, del Valle E and Laussy F P 2018 *Sci. Rep.* **8** 6975
[67] Glauber R J 1963 *Phys. Rev. Lett.* **10** 84
[68] Loudon R 2000 *The Quantum Theory of Light* 3rd edn (Oxford: Oxford University Press)

[69] Dalibard J and Reynaud S 1983 *J. Phys. France* **44** 1337

[70] López Carreño J C and Laussy F P 2016 *Phys. Rev. A* **94** 063825

[71] Mandel L 1982 *Phys. Rev. Lett.* **49** 136

[72] Vogel W 1991 *Phys. Rev. Lett.* **67** 2450

[73] Vogel W 1995 *Phys. Rev. A* **51** 4160

[74] Slusher R E, Hollberg L W, Yurke B, Mertz J C and Valley J F 1985 *Phys. Rev. Lett.* **55** 2409

[75] McCormick C F, Boyer V, Arimondo E and Lett P D 2007 *Opt. Lett.* **32** 178

[76] McCormick C F, Marino A M, Boyer V and Lett P D 2008 *Phys. Rev. A* **78** 043816

[77] Raizen M G, Orozco L A, Xiao M, Boyd T L and Kimble H J 1987 *Phys. Rev. Lett.* **69** 198

[78] Lu Z H, Bali S and Thomas J E 1998 *Phys. Rev. Lett.* **81** 3635

[79] Ourjoumtsev A, Kubanek A, Koch M, Sames C, Pinkse P W H, Rempe G and Murr K 2011 *Nature* **474** 623

[80] Schulte C H H, Hansom J, Jones A E, Matthiesen C, Gall C L and Atatüre M 2015 *Nature* **525** 222

[81] Zubizarreta Casalengua E, López Carreño J C, Laussy F P and del Valle E 2018 In preparation

[82] Zubizarreta Casalengua E, López Carreño J C, del Valle E and Laussy F P 2017 *J. Math. Phys.* **58** 062109

[83] Carmichael H J, Brecha R J and Rice P R 1991 *Opt. Commun.* **82** 73

[84] Bamba M, Imamoglu A, Carusotto I and Ciuti C 2011 *Phys. Rev. A* **83** 021802(R)

[85] Liew T C H and Savona V 2010 *Phys. Rev. Lett.* **104** 183601

[86] Jakeman E, Oliver C J and Pike E R 1975 *Adv. Phys.* **24** 349

[87] Yuen H P and Shapiro J H 1979 *Opt. Lett.* **4** 334

[88] Bondurant R S and Shapiro J H 1984 *Phys. Rev. D* **30** 2548

[89] Loudon R 1984 *Opt. Commun.* **49** 24

[90] Loudon R 1984 *Opt. Commun.* **49** 67

[91] Kitagawa M and Yamamoto Y 1986 *Phys. Rev. A* **34** 3974

[92] Collett M J, Loudon R and Gardiner C W 1987 *J. Mod. Opt.* **34** 881

[93] Xu X W and Li Y 2014 *Phys. Rev. A* **90** 033832

[94] Fischer K A, Müller K, Rundquist A, Sarmiento T, Piggott A Y, Kelaita Y A, Dory C, Lagoudakis K G, Müller K and Vuckovic J 2016 *Nat. Photon.* **10** 163

[95] Müller K, Fischer K A, Dory C, Sarmiento T, Lagoudakis K G, Rundquist A, Kelaita Y A and Vučković J 2016 *Optica* **3** 931

[96] Dory C, Fischer K A, Müller K, Lagoudakis K G, Sarmiento T, Rundquist A, Zhang J L, Kelaita Y, Sapra N V and Vuckovic J 2017 *Phys. Rev. A* **95** 023804

[97] Fischer K A, Kelaita Y A, Sapra N V, Dory C, Lagoudakis K G, Müller K and Vuckovic J 2017 *Phys. Rev. Appl.* **7** 044002

[98] López Carreño J C, Zubizarreta Casalengua E, Laussy F P and del Valle E 2018 arXiv:1806.08774

[99] del Valle E, Laussy F P and Tejedor C 2009 *Phys. Rev. B* **79** 235326